

DESIGN GUIDELINES FOR SHS THIN-WALLED COLUMNS WITH LARGE HOLES AT THEIR EXTREMITIES

Marios-Zois Bezas, Maxime Vermeylen, Helene Morch, Koenraad Ginckels, Jean-François Demonceau

Thin-walled cold-formed hollow columns are widely used in steel structure construction due to their advantages such as high strength, ductility and lightweight. When bolted connections are used, long bolts passing through the entire hollow cross-section are required. An alternative solution could be that large holes are made in one of the column faces, at the level of the connections, allowing thus the hand tightening of 'short' classical bolts. This paper investigates the influence of these holes on the resistance and stability of the column and aims at determining a safe way to compute the resistance of cross-sections and the stability of members in the presence of handholes. More specifically, square hollow sections (SHS) with large holes have been considered and their behaviour has been studied numerically using shell finite elements, accounting for local and distortional effects as well as material and geometrical non-linearities. Then, the obtained results have been compared with the predictions obtained through the code provisions for cross-section resistance and member buckling, in order to check their adequacy.

Keywords : thin-walled hollow sections; cross-section resistance; member buckling; EN 1993-1-3

1 Introduction

Thin-walled cold-formed steel elements represent a very attractive structural solution due to their fast manufacturing and erection on-site, as well as their high strength and ductility combined with a lightweight. These sections are extensively used as both primary or secondary structural elements in buildings, storage system structures or steel houses. The design of cold-formed steel joints is governed by two main problems: (a) the stability issues and (b) the selection of the connecting technology. The former is dominant for the design criteria while the latter could appear as purely technical, while it may sometimes strongly affect the structural behaviour and the design details of the elements.

When hollow sections are used for the columns of these structures, the beams could either welded or bolted to them. Although design provisions provide guidance on the determination of the weld strength, the design is generally limited and requires considerable workmanship, quality and inspection to determining if a weld is an appropriate connection method. In the case of bolted connections, long bolts all along the column's section width are required. An alternative solution could be that large holes are used at the level of the connections, thus allowing the tightening of shorter bolts by hand. These bolts are common ones and can be found much easier than the longer ones that sometimes should be produced on demand, an aspect that increases both the time and the cost of the structure. In addition, using long bolts, there is always the risk to provoke a local deformation of the

column face, especially for thin-walled sections covered in the present study: the more the bolt tightens in order to provide an adequate contact of the elements, the more the risk of local failure of the column face increases. Besides that, in some countries, this joint configuration is not acceptable by the inspection committees. Therefore, the use of the handholes at the connection level's looks to be a good structural solution.

Although a lot of studies on SHS thin-walled columns have been performed by various researchers, they are mainly focusing on members with full hollow sections, i.e., without handholes. Toffolon et al. [1] studied experimentally and numerically the local and interactive buckling phenomena, and in [2], they provided design recommendations for the buckling resistance of cold formed SHS members. Yun et al. [3] and Li et al. [4] investigated the influence of the steel grade and of the residual stresses respectively on the resistance of square hollow members. In the framework of the recently finished RFCS European project with the acronym HOLLOSSTAB [5] which involved numerical and experimental investigations considering various hollow cross-sections and steel grades, design rules and recommendations for the verification of the cross-sectional and member stability and capacity have been provided. On the contrary, studies focusing on square hollow members with holes are very limited. Singh et al. [6] examined numerically the effects of various hole shapes (i.e. circular, square, hexagonal) and sizes on the buckling behaviour of cold-formed and hotrolled steel stub columns. Devi et al. [7] studied experimentally and numerically the torsional behaviour of cold-formed steel square hollow section members without holes or with holes all along the member's length.

The objective of this paper is to investigate the influence of the handholes on the response of the columns and to determine a safe way to compute the resistance of cross-sections and the stability of members in the presence of handholes. To achieve this, a large number of parametrical numerical studies on SHS columns subjected to compression or compression and bending have been conducted with ABAQUS software [8] using shell elements. As a first step, members without handholes have been considered and their numerically obtained resistances were compared with the analytical ones given in the codes; the latter have been recently validated in HOLLOSSTAB [5] project through experimental tests. This step consists a validation of the software and proves its adequacy to be used for the parametric/comparative study. Then, the numerical resistances of members with handholes have been compared with analytical ones obtained by applying the provisions of the existing codes. In Europe, the design of hollow thin-walled columns is carried out using mainly EN 1993-1-3 [9] which is dedicated to the design cold-formed profiles, with references to EN 1993-1-1 [10] and EN 1993-1-5 [11] when relevant. Therefore, comparisons are here made with the resistances evaluated in accordance with EN 1993-1-3; references are also made to the provisions of its forthcoming version prEN 1993-1-3 [12] only when those differ from the provisions of the former. Finally, the adequacy of the existing design rules is checked and recommendations in line with EN 1993-1-3 for the design of such structural elements are provided.

These studies are part of the ongoing project funded by SPW (Service public de Wallonie) project entitled ACTIONS: 'Advanced Eurocodes Compliant Tools for Industrial Optimized Innovative Structures', involving STOW group, GDTech and CRM companies, as well as the University of Liège.

2 Finite-element modelling

All the numerical models for the parametrical numerical studies presented in this article were created with ABAQUS non-linear finite element software using isoparametric shell elements with reduced integration (i.e. type S4R). The samples have been modelled as pin-ended at their extremities at the centre of gravity of the full section, where fictitious end plates have been introduced through a specific constraint, so as to distribute uniformly the external applied loads on the cross-section but also to avoid any local failure at the load application point (see Fig. 1).

In all simulations, the following two steps were applied. First, a linear buckling analysis (LBA) was performed in order to obtain both local and global elastic critical loads as well as their eigenshapes. These eigenshapes were then used, separately or combined, as initial imperfection shapes within the second simulation step, where a full nonlinear analysis (GMNIA) was carried out in order to obtain the maximum load carrying capacity of the column; in these simulations, the applied load increases up to failure of the member.

For all simulations, the steel grade HX420LAD was set constant and an elastoplastic material behaviour law with strain hardening in accordance to EN 1993-1-5 has been adopted. Based on the provisions of prEN 1993-1-3 [12] and EN 10346 [13], its basic yield strength is equal to $f_{yb} = 400\text{N/mm}^2$.

For the GMNIA intended to reach the cross-sectional resistance (i.e. simulations where the member slenderness is lower than 0.2 – see §3.1), an equivalent local imperfection equal to $h/400$ (h is the width of the cross-section) with shape affine to the first local elastic instability mode has been used. This value shows the best agreement with the design curve (Winter's curve) for local buckling given in EN 1993-1-5. This assumption, validated by the HOLLOSSTAB project and supported by existing literature [14, 15], aligns with experimental findings.

For the GMNIA intended to reach the buckling resistance of the member (i.e. simulations with intermediate-to-high member slenderness), the following two initial imperfections have been implemented: (i) an equivalent global imperfection equal to $L/1000$ (L being the member length) with shape affine to the first global elastic instability mode and (ii) an equivalent local imperfection equal to $h/400$ as explained above. Again, the selected combination of initial imperfections is in line with the outcomes of the HOLLOSSTAB project.

In the conducted parametric study, the profiles have been selected in order to cover a wide range of cross-section wall slenderness, while the member lengths were varied so as to account for both local and flexural buckling through the member slenderness range. Subsequently, numerical investigations on short and slender columns subjected to compression or compression and bending with or without handholes have been performed. For this study, the size of the handholes is assumed to be constant and equal to $140 \times 55\text{mm}$, as these dimensions are usually met in practice.

3 Cross-section resistance

For the study of the cross-section resistance, two different configurations have been considered: (i) short columns without handholes and (ii) short columns with a handhole at the mid-height. For the first configuration, a direct comparison with Eurocode may be contemplated as the latter covers such cases. For sake of simplicity, the section with the handhole will be named hereafter as ‘cut section’. For both configurations, the load is implemented at the centre of gravity of the SHS full cross-section while, for the second configuration, an additional loading case has been considered where the load is introduced on one of the column faces, as explained in §3.2.3.

3.1 RESISTANCE OF FULL CROSS-SECTION

Tab 1 presents the details of the full cross-sections that have been considered as well as their numerically and analytically determined resistances under pure compression. To prevent flexural buckling, the length of the samples was selected in such a way that $\bar{\lambda} = \sqrt{N_{c,Rk}/N_{cr}} \leq 0.2$, a member slenderness below which the European buckling curves assume that no reduction associated with buckling is required. The numerical resistance ($N_{ult,n}$) corresponds to the maximum failure load, while the analytical one may be determined as follows [9, 12]:

$$N_{c,Rk} = \begin{cases} A \cdot f_{yb} & \text{if } A_{eff} = A \\ A_{eff} \cdot f_{yb} & \text{if } A_{eff} < A \end{cases} \quad (1)$$

where the effective area A_{eff} is calculated according to EN 1993-1-3, accounting only for local buckling phenomena as distortion is not relevant for closed sections. EN 1993-1-3 refers directly to EN 1993-1-5 as far as local buckling is concerned; except for the definition of the width term which EN 1993-1-3 considers as equal to $\bar{b} = b_p = h - t$, a value which differs from both EN 1993-1-5 and prEN 1993-1-1, where \bar{b} should be taken equal to $h/3t$ for the SHS sections. In the following, the provision of EN 1993-1-3 (i.e. $\bar{b} = h - t$) has been applied, as the considered SHS profiles are cold-formed ones. Therefore, the buckling factor given in EN 1993-1-5, Table 4.1, is $k_\sigma = 4$ and the reduction factor is $\rho = (\bar{\lambda}_p - 0.22)/\bar{\lambda}_p^2$. It can be easily seen from Tab. 1 that both numerical and analytical resistances are quite similar with a mean value of the ratio $n = N_{ult,n}/N_{c,Rk}$ equal to 1.01 with a CoV of 1.4%.

Fig. 2 presents the numerically determined reduction factor $\rho_{num} = N_{ult,n}/N_{pl}$ versus the plate slenderness (corresponding to the plate slenderness of an internal plate). The very good agreement between the numerical results and the buckling design curve of EN 1993-1-5 can be easily observed. It can be therefore concluded that the numerical model predicts the design resistance of these sections with high accuracy, while the selected values of the initial imperfections and the material law are suitable. These results appear as a validation of the ABAQUS simulations.

3.2 RESISTANCE OF THE CUT CROSS-SECTION

In order to check the resistance of the cut section, the same samples as in §3.1 were assumed but with a handhole at their mid-height; two loading cases were also considered.

3.2.1 CASE 1: CENTRALLY LOADED SHORT COLUMNS

Despite the fact that the member is subjected to an axial load at the centre of gravity G of the full section, at the position of the handhole, a bending moment appears due to the eccentricity of the point application of the load (i.e. G) and the centroid of the cut and/or the effective section (i.e. G_1 and G_2 , see Fig. 3). Thus, the cut section should be checked against $N_{Ed} + M_{Ed,z}$, and the following formula may be used:

$$\frac{N_{Ed}}{N_{c,Rk}} + \frac{M_{z,Ed} + \Delta M_{z,Ed}}{M_{c,Rk}} \leq 1.0 \quad (2)$$

To compute the design resistances of the cut section according to Eq. (2), the procedure of EN 1993-1-3 is followed, where the upper and the bottom flanges with the edge folds are treated as stiffeners and both local and distortional buckling are accounted for. Local buckling is covered by the provisions of EN 1993-1-5 while distortional buckling by EN 1993-1-3. In addition, according to EN 1993-1-3, the effective cross-sectional area A_{eff} should be determined by assuming that the cross-section is subjected only to uniform stresses due to axial compression in its centre of gravity G_1 , while for the calculation of the effective section modulus W_{eff} , the member is subjected only to bending.

Fig. 4 presents (in blue) the ratio of the numerically determined resistance of the cut section to its analytical one versus the plate slenderness (corresponding to the plate slenderness of a wall without a hole). The numerical resistance ($N_{ult,n}$) is determined as the maximum failure load, while the analytical one (N_{anal}) is derived as the maximum axial load that satisfies Eq. (2). The mean value (solid blue line) of the ratio $N_{ult,n}/N_{anal}$ is equal to 1.23 with a CoV (dotted blue line) of 15%. It can be seen that the analytical resistance is always on the safe side, with the most conservative results being for the slenderest sections. It should be mentioned that the analytical resistances have been evaluated with the simplified method that Eurocode follows, where the effective properties are calculated apart for cross-section subjected only to compression or only to bending. This method is easier to be applied in practice but the stress distribution used for the calculation does not reflect the actual one. When the actual stress distribution is used (green points in Fig. 4), again the predicted resistances are on the safe side. For low-to-intermediate slenderness, the predictions are close to the ones evaluated with the simplified procedure given in Eurocode 3, while for the slenderest ones, the consideration of the actual stresses seems to be even more conservative. This could be explained by the fact that the plates in risk of local instability to which the EN 1993-1-1 classification rules apply are assumed to be infinitely long, while here it is not the case, as the length of the holes is rather small. Subsequently, the actual boundary conditions of the plates located along the holes are more rigid than considered in the code. For low slenderness, the effect is negligible as the instability is limited and the failure is reached mostly by yielding. But the higher the slenderness, the higher the instability effects, and the assumption of “infinitely long plates” becomes then more conservative. Although it has been demonstrated that the simplified procedure given in EN 1993-1-3 provides safe results, some further investigations should be carried out in the future regarding the conservative character appearing at the intermediate-to-higher range of slenderness.

It should be also mentioned that according to EN 1993-1-3, for profiles where there is no reduction to their area, the value of the average yield strength f_{ya} accounting for work hardening due to cold forming can be used to determine the resistance instead of the basic one f_{yb} . However, as the majority of the considered profiles are thin-walled ones and so they are prone to local buckling, the beneficial effect

of the use of f_{ya} is negligible; it can be applied only for two of the considered specimens and gives less conservative results almost by 2%.

3.2.2 CASE 2: ECCENTRICALLY LOADED SHORT COLUMNS

Although the beam could be bolted on all the column faces except the one with the handhole, it has been selected here to check the cross-sectional resistance with an eccentricity $e_z = (h - t)/2$ (see Fig. 3 for the axis definition), as an eccentricity in y -axis is anyway developed due to the cut/effective cross-section. Being so, the cut section is subjected to an axial force and biaxial bending and so its resistance should be checked, according to Eurocode 3 Part 1–3, using the following formula:

$$\frac{N_{Ed}}{N_{c,Rk}} + \frac{M_{y,Ed}}{M_{cy,Rk}} + \frac{M_{z,Ed} + \Delta M_{z,Ed}}{M_{cz,Rk}} \leq 1.0 \quad (3)$$

Fig. 5 presents the ratio of the numerically determined resistance of the cut section to the analytical one, again versus the plate slenderness of a wall without a hole. The numerical resistance corresponds to the maximum failure load and the analytical one is derived as the maximum axial load that satisfies Eq. (3). EN 1993-1-3 was again followed for the calculation of effective sectional properties. Once more, the analytically determined resistance is safe with a mean value of the ratio $N_{ult,n}/N_{anal}$ equal to 1.12 and a CoV of 4.8%.

4 Critical buckling load

For centrally loaded columns with doubly symmetric section, two global buckling modes (flexural, torsional) may occur; their critical loads can be analytically determined according to the technical report CEN/TR 1993-1-103 [16]. Although local buckling is also relevant for thin-walled elements, this phenomena is not explicitly considered in the design procedure proposed in the Eurocodes but is accounted for through the effective properties of the cross-sections. This contrasts with the American code [17] and the well-known Direct Strength Method (DSM) for cold-formed profiles [18].

The investigations focused here on the influence of the handholes on the flexural critical load as torsional buckling are not deemed to occur in hollow sections. For these numerical and analytical investigations, ten different profiles with a member slenderness varying from 0.599 to 2.074 (see Tab. 2) have been contemplated with three different member layouts as it is illustrated in Fig. 6. The case without any handhole along the member aims first to validate the software through comparisons with the elastic critical loads given in EN 1993-1-103 [16]. Secondly, it is used as the reference value to which all the critical loads obtained for the members with handholes are compared.

Tab. 2 summarises the numerical results for members with no handholes, 1 and 2 handholes at each extremity. For cases H₂ and H₄, both numerical critical loads along y - and z -axis (i.e. $N_{cr,n,y}$ and $N_{cr,n,z}$, see Fig. 6 for the definition of the axis in regard to the position of the handhole) are reported as well as the ratios (n_y and n_z) of these loads over the analytical flexural critical load $N_{cr,F,an}$ of the gross cross-section.

Through these numerical simulations and comparisons, the following conclusions may be drawn.

- Both the numerical and the analytical flexural critical loads for members with gross cross-sections are quite similar, with a mean value of the ratio $N_{cr,num}/N_{cr,F,an}$ equal to 0.99 and a COV 0.95%; the higher differences appear for the thicker profiles but are rather low (less than 3%).
- Due to the presence of the handholes along the member's length, there is no more a pure flexural buckling mode but a combination of flexural buckling with a slight presence of local buckling around the holes.
- Although this local buckling is more pronounced in $N_{cr,n,y}$ than in $N_{cr,n,z}$ (critical loads along y - and z -axis, respectively, see Fig. 6 for the definition of the axis in regard to the position of the handhole), it however remains rather limited;
- The existence of the handholes at the extremities reduces the critical load by 1–3% compared to the full cross-section flexural critical load; this difference seems as rather small and its impact to the ultimate buckling resistance of the member is negligible.

5 Buckling resistance

The validity and accuracy of the formulae for buckling resistance of members subjected to compression or compression and bending given in both EN 1993-1-3 and prEN 1993-1-3 are checked in the following against numerical results where the influence of the handholes is accounted for. Differences between both versions of the norm are found only for members subjected to compression and bending, where new equations are provided in prEN 1993-1-3. However, both sets are based on a second order in-plane theory and rely on several common aspects, such as the equivalent moment concept, the definition of buckling length, and the amplification concept.

5.1 BUCKLING RESISTANCE OF MEMBERS WITHOUT HANDHOLES

5.1.1 MEMBERS SUBJECTED TO COMPRESSION

Tab. 3 presents the details of the samples that have been considered as well as their numerically and analytically determined buckling resistances to pure compression. The samples have been selected so as to cover a wide range of member slenderness where both local and global instabilities are relevant. The analytical resistance is given by the expression [9, 12]:

$$N_{b,Rk} = \begin{cases} \chi \cdot A \cdot f_{yb} & \text{if } A_{eff} = A \\ \chi \cdot A_{eff} \cdot f_{yb} & \text{if } A_{eff} < A \end{cases} \quad (4)$$

where the effective area A_{eff} is calculated according to EN 1993-1-3. The value of the buckling reduction factor χ is computed using buckling curve b in combination with the basic yield stress f_{yb} according to EN 1993-1-3. The use of buckling curve b is in line with the recommendations of the CIDECT [19], is on the safe side compared to buckling curve a that has been justified in HOLLOSSTAB project and is less conservative than EN 1993-1-1 where buckling curve c is proposed for cold-formed sections.

It can be thus easily seen from Tab. 3 that there is good agreement between the numerical resistances and the ones calculated according to EN 1993-1-3, with code provisions being always on the safe side; the mean value of the ratio $n = N_{ult,n}/N_{b,Rk}$ is equal to 1.10 with a deviation of 6.7%.

Fig. 7 shows the numerically determined reduction factor $\chi_{\text{num}} = N_{\text{ult},n}/(A_{\text{eff}}f_{yb})$ versus the global flexural slenderness; relevant buckling curves given in EN 1993-1-1 are illustrated too. It can be easily seen that all the results are above curve *b*. Subsequently, the numerical model appropriately predicts the buckling resistance of SHS full section members, while the selected values for the initial imperfections, the material law and the buckling curve are justified.

5.1.2 MEMBERS SUBJECTED TO COMPRESSION AND BENDING

For the verification of the buckling resistance of the members subjected to combined compression and bending, both EN 1993-1-3 and prEN 1993-1-3 are used in the following. According to EN 1993-1-3, the buckling resistance of members subjected to axial compression and bending should satisfy the interaction equations given in EN 1993-1-1 – clause 6.3.3(4), while in prEN 1993-1-3, the new interaction equations below are proposed:

$$\begin{aligned} & \left(\omega_{x,y} \frac{N_{Ed}}{\chi_y N_{c,Rk}} \right)^{\alpha_y} \\ & + \left(\omega_{x,LT} \frac{M_{y,Ed} + \Delta M_{y,Ed}}{\chi_{LT} M_{cy,Rk}} \right)^{\beta_y} \\ & + \left(\frac{M_{z,Ed} + \Delta M_{z,Ed}}{M_{cz,Rk}} \right)^{\delta_y} \leq 1.0 \end{aligned} \quad (5)$$

$$\begin{aligned} & \left(\omega_{x,z} \frac{N_{Ed}}{\chi_z N_{c,Rk}} \right)^{\alpha_z} \\ & + \left(\omega_{x,LT} \frac{M_{y,Ed} + \Delta M_{y,Ed}}{\chi_{LT} M_{cy,Rk}} \right)^{\beta_z} \\ & + \left(\frac{M_{z,Ed} + \Delta M_{z,Ed}}{M_{cz,Rk}} \right)^{\delta_z} \leq 1.0 \end{aligned} \quad (6)$$

The interpolation factors $\omega_{x,i}$ depend on the location of the cross-section under consideration and account for the relevant buckling mode and axial force or bending moment; they are equal to 1.0 according to Table 8.10 of prEN 1993-1-3 as the member is simply supported (most loaded section at the middle). The exponents of the interaction formulae α_i , β_i , and δ_i are equal to $\chi_i/\omega_{x,i} \geq 0.85$; more details are provided in prEN 1993-1-3.

The same samples as in section 5.1.1 have been considered but in this case the load is applied with an eccentricity $e_z = (h - t)/2$ (see Fig. 3 for the axis definition). Tab. 4 summarises the details of the studied members as well as their numerically and analytically determined resistances. The numerical resistance ($N_{\text{ult},n}$) corresponds to the maximum axial failure load, $N_{\text{anal},EC3}$ is derived as the maximum axial load that satisfies equations (6.61)-(6.62) or EN 1993-1-1 and $N_{\text{anal},prEC3}$ is derived as the maximum axial load that satisfies Eqs. (5) and (6) of this paper. The ratios $n_{EC3} = N_{\text{ult},n}/N_{\text{anal},EC3}$ and $n_{prEC3} = N_{\text{ult},n}/N_{\text{anal},prEC3}$ are reported too. For the calculation of the effective properties EN 1993-1-3 was followed, while method 2 for members not susceptible to torsional deformations is used for the determination of the k_{yy} factor. Method 2 (Annex B of EN 1993-1-1) is based on the concept of global factors, in which simplicity prevails against transparency. This approach appears to be the more straightforward in terms of a general format and is mainly focused on the direct design of standard cases; however it is only applicable for I, RHS and SHS sections. Therefore, where the equivalent uniform moment factor C_{my} is equal to 1.0 for constant moment diagram.

$$k_{yy} = C_{my} \left(1 + 0.6 \bar{\lambda}_y \frac{N_{Ed}}{\frac{Z_y N_{Rk}}{\gamma_{M1}}} \right) \leq C_{my} \left(1 + 0.6 \frac{N_{Ed}}{\frac{Z_y N_{Rk}}{\gamma_{M1}}} \right)$$

Fig. 8 shows the ratios of the ultimate numerically obtained buckling resistances over the analytical ones calculated for both EN 1993-1-3 and prEN 1993-1-3 versus the global flexural slenderness. It can be seen that both code provisions are on the safe side and they provide globally similar results. The mean value of the ratio $N_{ult,n}/N_{anal}$ is equal to 1.11 for both normative documents, with prEN 1993-1-3 to have a slightly bigger scatter (5.4%) compared to EN 1993-1-3 (4.1%). Again, the numerical model appropriately predicts the buckling resistance of SHS full-section members subjected to compression and bending.

5.2 BUCKLING RESISTANCE OF A MEMBER WITH HANDHOLES

In order to check the influence of the handholes on the buckling resistance of these members, the same samples reported in the previous section were considered, and for each member, two configurations have been adopted: members with 1 handhole per extremity and members with 2 handholes per extremity, named H₂ and H₄ in Fig. 6, respectively. Again, in terms of loading, two cases are distinguished: centrally and eccentrically loaded columns.

5.2.1 CENTRALLY LOADED MEMBERS

Fig. 9 compares the ultimate buckling resistance of the members with handholes obtained numerically (1 or 2 holes at each extremity) to the numerical resistance of the same members but without handholes versus their global flexural slenderness. The comparisons are limited to slenderness higher than 0.7 where a member failure occurs, as for lower slenderness, the specimen reaches the cross-sectional resistance of the cut section. As shown, the influence of the handholes on the buckling resistance of the member is limited (differences less than 6%).

Fig. 10 presents the ratio of the numerically determined resistance of the member to the analytical one versus the global flexural slenderness. The analytical resistance is $N_{anal} = \min\{N_{b,Rk}, N_{c,Rk}\}$, where $N_{b,Rk}$ is the buckling resistance of the member assumed without handholes given by (Eq. (4)) and $N_{c,Rk}$ is the cross-section resistance of the cut cross-section as explained in §3.2.1. The mean value of the ratio $N_{ult,n}/N_{anal}$ is equal to 1.12 and 1.11 for specimens with 1 hole/extremity and 2 holes/extremity respectively; CoV is 8.6% and 8.8% correspondingly. Furthermore, the analytically determined resistance is on the safe side for all specimens.

5.2.2 ECCENTRICALLY LOADED MEMBERS

As in section 3.2.2, the load is introduced with an eccentricity $e_z = (h - t)/2$. For this loading case too, it has been found that the influence of the handholes to the ultimate buckling resistance of the member as this has been evaluated for members without handholes, is limited (differences less than 2.4%, see Fig. 11).

Figs. 12 and 13 present the ratio of the numerically determined resistance of the member to the analytical one versus the global flexural slenderness. The analytical resistance is equal to $N_{anal} = \min\{N_{b,Rk}, N_{c,Rk}\}$, where $N_{b,Rk}$ is the buckling resistance of the member without accounting for the

handholes at the extremities in accordance with EN 1993-1-3 and prEN 1993-1-3, while $N_{c,Rk}$ is the cross-section resistance of the cut section as explained in §3.2.2. It can be easily seen that the analytically determined resistance is on the safe side for all specimens and for both considered standards. In addition, for both configurations of handholes and both normative documents, the mean value of the ratio $N_{ult,n}/N_{anal}$ is equal to 1.11 with a CoV of about 4.2% and 5.0% for the provisions of EN 1993-1-3 and prEN 1993-1-3 respectively. Although for some cases both standards provide slightly different results, the global tendency is the same, with prEN 1993-1-3 being slightly less conservative than EN 1993-1-3 in the range of medium-to-high slenderness.

6 Conclusions

The paper investigates the influence of large holes used at the extremities of SHS thin-walled columns to allow an easy tightening of bolts by hand on their resistance and stability. More specifically, the behaviour of these elements has been studied numerically by means of ABAQUS software using shell elements, accounting for both local and distortional effects, as well as material and geometrical non-linearities. The results have been then compared with analytical ones obtained by applying the provisions of EN 1993-1-3, which is dedicated to the design of cold-formed profiles, for cross-section resistance and member buckling; comparisons are also made to the provisions of its forthcoming version prEN 1993-1-3 when these ones differ from the provisions of the former. Through these studies, involving numerical and analytical aspects, the following conclusions may be drawn.

- The existence of the handholes at the member's extremities reduces the elastic critical buckling load by 1–3% compared to the full cross-section elastic flexural critical load; this difference appears as rather small and its impact to the ultimate buckling resistance of the member is limited.
- Due to the presence of the handholes along the member's length, there is no more a pure flexural buckling mode but a combination of flexural buckling with a slight presence of local buckling around the holes.
- The generic rules proposed in the current version of EN 1993-1-3 (or the new version, namely, prEN 1993-1-3, which differs from the EN version only for member buckling resistance under compression and bending) can be safely used to calculate the cross-sectional resistance of columns with handholes subjected to compression and mono-axial or biaxial bending.
- The influence of the handholes at the extremity of members to their ultimate buckling resistance under compression or compression and bending is rather limited.
- Despite the differences in the proposed formulae, the provisions of both EN 1993-1-3 and prEN 1993-1-3 provide quite similar resistances for members subjected to axial force and bending moments.

Therefore, the design resistance of pin-ended SHS columns with large holes at their extremities could be determined as the minimum one of (i) the cross-section resistance of the cut section according to EN 1993-1-3/prEN 1993-1-3 where both local and distortional buckling are accounted for and (ii) the

buckling resistance of the member according to EN 1993-1-3/prEN 1993-1-3 by neglecting the handholes.

Nomenclature

The notations used in the paper are listed below and are in line with the ones given in Eurocode 3.

Latin upper-case symbols

A	Cross-sectional area
A_{eff}	Effective area of a cross-section
C_{my}	Equivalent uniform moment factor
E	Young's modulus of elasticity
L	Length of the member
M_{cr}	Elastic critical bending moment based on the gross cross-sectional properties
$M_{y,\text{Ed}}, M_{z,\text{Ed}}$	Bending moment about $y - y$ and $z - z$ axis respectively
$M_{y,\text{Rk}}, M_{z,\text{Rk}}$	Characteristic value of the resistance to bending moment about $y - y$ and $z - z$ axis respectively
$N_{\text{b,Rk}}$	Characteristic value of the buckling resistance of a member in compression
N_{cr}	Elastic critical axial force for the relevant buckling mode based on the gross cross-sectional properties
$N_{\text{cr,F}}$	Elastic critical axial force for flexural buckling
$N_{\text{cr,l}}$	Elastic critical axial force for local buckling
$N_{\text{c,Rk}}$	Characteristic value of the resistance to compression axial force
$N_{\text{cr,T}}$	Elastic critical axial force for torsional buckling
N_{Ed}	Axial force
N_{pl}	Design value of the plastic resistance to axial force of the gross cross-section
N_{ult}	Ultimate test resistance to axial force of the cross-section
$W_{\text{eff,y}}, W_{\text{eff,z}}$	Elastic section modulus of the effective area of a cross-section for bending about $y - y$ and $z - z$ axis, respectively
R	External radius of the corner

Latin lower-case symbols

\bar{b}	Appropriate width, that is equal to h for angle sections according to EN 1993-1-5
c	Outstand flange width ($c = h - t - r$)

e_0	Distance between the gravity centre of the cut and the full cross-section
e_N	Shift of the centroid of the effective cross-section relative to the centroid of the gross cross-section
f_y	Yield strength
f_{ya}	Average yield strength, accounting for work hardening due to cold forming
f_{yb}	Basic yield strength
h	Width of the cross-section
k_{ij}	Interaction factors for uniform members in bending and axial compression
k_σ	Plate buckling coefficient
r	Internal radius of the corner
t	Thickness of the cross-section

Greek upper-case symbols

ΔM_{Ed}	Additional bending moment resulting from the shift of the centroid of the effective cross-section relative to the centroid of the gross cross-section
-----------------	---

Greek lower-case symbols

α	Imperfection factor
α_{LT}	Imperfection factor for lateral torsional buckling
ε	Material parameter depending on f_y
$\bar{\lambda}$	Relative slenderness for flexural buckling
λ_{LT}	Relative slenderness for lateral torsional buckling
$\bar{\lambda}_p$	Relative plate slenderness for plate buckling
ρ	Reduction factors for plate buckling
$\sigma_{cr,l}$	Elastic critical plate buckling stress
χ_{LT}	Reduction factor for lateral torsional buckling
χ_φ	Reduction factor due to flexural buckling
ψ	Ratio of end moments in a segment of beam, stress ratio, angle
ω_{ij}	Interpolation factors in the design stability check of members in combined bending and compression

Acknowledgements

The authors of this publication acknowledge the Walloon Region, Logistics in Wallonia ASBL and Pôle MecaTech for their support in the framework of the project N°8528 entitled ACTIONS 'Advanced Eurocodes Compliant Tools for Industrial Optimized Innovative Structures'.

Partners of the project are STOW group, GDTech and CRM companies, as well as the University of Liege.

Tables

Tab. 1 Resistance of full cross-sections subjected to pure compression

No	Cross-section	L [mm]	$\bar{\lambda}_p$ [–]	ρ [–]	A_{eff} [mm ²]	$N_{c,Rk}$ [kN]	$N_{ult,n}$ [kN]	ρ_{num} [–]	n [–]
1	SHS 140×2	1000	1.584	0.544	590	236.0	236.3	0.540	1.00
2	SHS 140×3	800	1.048	0.754	1216	486.4	494.5	0.763	1.02
3	SHS 140×5	600	0.620	1.000	2636	1054	1039.0	0.986	0.99
4	SHS 120×2	590	1.354	0.618	574	229.4	229.8	0.615	1.00
5	SHS 120×4.5	590	0.589	1.000	2027	810.7	807.5	0.996	1.00
6	SHS 120×5.5	590	0.478	1.000	2441	976.4	994.6	1.019	1.02
7	SHS 100×2	500	1.125	0.715	550	220.2	225.8	0.729	1.03
8	SHS 100×3	500	0.742	0.948	1080	432.1	439.0	0.962	1.02
9	SHS 100×5	500	0.436	1.000	1836	734.2	756.9	1.031	1.03
10	SHS 150×2	500	1.699	0.512	596	238.6	244.7	0.521	1.03
11	SHS 150×3.5	600	0.961	0.802	1614	645.7	670.5	0.830	1.04
12	SHS 150×6	500	0.551	1.000	3363	1345.3	1353.0	1.006	1.01
13	SHS 160×2	640	1.813	0.485	602	240.9	244.0	0.487	1.01
14	SHS 160×3	640	1.201	0.680	1258	503.2	506.3	0.680	1.01
15	SHS 160×4.5	640	0.793	0.911	2498	999.2	1033.0	0.940	1.03

Tab. 2 Flexural critical load: numerical results for members with 0, 1 and 2 handholes at each extremity

No	Cross-section	L [mm]	$N_{cr,Fan}$ [kN]	$N_{cr,num}$ [kN]	H2				H4			
					$N_{cr,nx}$ [kN]	n_y [–]	$N_{cr,nz}$ [kN]	n_z [–]	$N_{cr,nx}$ [kN]	n_y [–]	$N_{cr,nz}$ [kN]	n_z [–]
1	SITU 140×2	7000	146.1	145.47	145.5	1.00	145.3	0.99	145.4	0.99	145.2	0.99
2	SITU 140×3	5000	417.4	413.86	413.7	0.99	412.8	0.99	413.1	0.99	411.6	0.99
3	SITU 140×5	3000	1821.9	1784.7	1782.0	0.98	1763.6	0.97	1769.7	0.97	1742.5	0.96
4	SITU 120×2	4800	193.8	192.55	192.5	0.99	191.9	0.99	192.1	0.99	191.2	0.99
5	SITU 120×5.5	2000	2722.7	2636.5	2620.9	0.96	2515.0	0.92	2550.0	0.94	2425.6	0.89
6	SITU 100×2	3300	234.1	231.97	231.6	0.99	228.4	0.98	229.7	0.98	225.2	0.96
7	SITU 100×5	2000	1407.7	1368.4	1357.5	0.96	1277.5	0.91	1307.9	0.93	1209.8	0.86
8	SITU 150×2	9000	109.2	108.64	108.6	1.00	108.6	1.00	108.6	0.99	108.6	0.99
9	SITU 150×6	3200	2321.8	2269.9	2267.3	0.98	2248.9	0.97	2255.1	0.97	2225.9	0.96
10	SITU 160×2	8500	149.0	148.26	148.3	0.99	148.2	0.99	148.2	0.99	148.1	0.99
11	SITU 160×4.5	3800	1574.1	1546.3	1545.3	0.98	1538.1	0.98	1540.8	0.98	1528.0	0.97

Tab. 3 Buckling resistance of full cross-section members subjected to pure compression

No	Cross-section	L [mm]	$N_{cr,F}$ [kN]	$N_{cr,local}$ [kN]	$\bar{\lambda}_p$ [–]	$\bar{\lambda}_F$ [–]	χ [–]	$N_{b,Rk}$ [kN]	$N_{ult,n}$ [kN]	n [–]
1	SHS 140×2	5000	286.4	174.4	1.58	0.91	0.656	154.9	170.9	1.10
2	SHS 140×2	7000	146.1	174.4	1.58	1.27	0.441	104.1	111.5	1.07
3	SHS 140×3	4000	652.1	590.1	1.05	0.86	0.684	332.9	360.8	1.08
4	SHS 140×3	5000	417.4	590.1	1.05	1.08	0.548	266.3	326.1	1.22
5	SHS 140×5	3000	1821.9	2744.8	0.62	0.76	0.748	789.0	921.4	1.17
6	SHS 120×2	3800	309.3	203.6	1.35	0.86	0.686	157.4	173.1	1.10
7	SHS 120×2	4800	193.8	203.6	1.35	1.09	0.543	124.5	136.1	1.09
8	SHS 120×5.5	2000	2722.7	4276.2	0.48	0.60	0.838	817.9	881.0	1.08
9	SHS 100×2	3300	234.1	244.6	1.13	0.97	0.616	135.7	168.3	1.24
10	SHS 100×5	1300	3331.9	3860.4	0.44	0.47	0.898	659.0	751.9	1.14
11	SHS 100×5	4500	278.1	3860.4	0.44	1.63	0.300	220.3	240.3	1.09
12	SHS 150×2	6500	209.3	162.7	1.70	1.07	0.555	132.4	135.6	1.02
13	SHS 150×2	9000	109.2	162.7	1.70	1.48	0.350	83.6	83.8	1.00
14	SHS 150×6	3200	2321.8	4433.0	0.55	0.76	0.748	1006.4	1121.0	1.11
15	SHS 150×6	2200	4912.2	4433.0	0.55	0.52	0.874	1175.4	1239.4	1.05
16	SHS 160×2	8000	168.2	152.5	1.81	1.20	0.480	115.6	115.8	1.00
17	SHS 160×4.5	3800	1574.1	1746.4	0.79	0.80	0.726	725.9	850.1	1.17

Tab. 4 Buckling resistance of members with full cross-section subjected to compression and bending according to EN 1993-1-3 & prEN 1993-1-3 and comparisons with numerical results

No	Cross-section	L [mm]	W_{eff} [mm ³]	M_{cr} [kNm]	χ_{LT} [–]	k_{yy} [–]	$N_{anal,EC3}$ [kN]	$N_{anal,prEC3}$ [kN]	$N_{ult,n}$ [kN]	n_{EC3} [–]	n_{prEC3} [–]
1	SHS 140×2	5000	36,283	350.26	0.99	1.28	79.5	79.3	86.79	1.09	1.09
2	SHS 140×2	7000	36,283	250.19	0.99	1.44	60.3	62.2	65.04	1.08	1.05
3	SHS 140×3	4000	63,451	641.57	1.00	1.24	157.0	156.1	185.41	1.18	1.19
4	SHS 140×3	5000	63,451	513.26	0.99	1.33	135.5	137.6	159.43	1.18	1.16
5	SHS 140×5	3000	118,418	1359.38	1.00	1.19	336.0	330.0	377.42	1.12	1.14
6	SHS 120×2	3800	28,257	287.99	1.00	1.25	77.5	76.5	84.95	1.10	1.11
7	SHS 120×2	4800	28,257	227.99	0.99	1.35	66.1	67.1	73.67	1.11	1.10
8	SHS 120×5.5	2000	93,016	1364.67	1.00	1.15	334.0	320.6	378.75	1.13	1.18
9	SHS 100×2	3300	21,031	189.83	0.99	1.29	67.0	67.3	74.78	1.12	1.11
10	SHS 100×5	1300	58,034	1088.80	1.00	1.11	263.5	260.1	294.94	1.12	1.13
11	SHS 100×5	4500	58,034	314.54	0.97	1.56	127.5	135.4	146.56	1.15	1.08
12	SHS 150×2	6500	40,293	403.79	1.00	1.35	72.5	73.2	75.96	1.05	1.04
13	SHS 150×2	9000	40,293	291.63	0.99	1.55	52.1	54.3	54.58	1.05	1.01
14	SHS 150×6	3200	161,178	1853.86	1.00	1.19	429.0	420.8	472.42	1.10	1.12
15	SHS 150×6	2200	161,178	2696.53	1.00	1.13	474.0	462.6	520.13	1.10	1.12
16	SHS 160×2	8000	44,041	328.67	0.99	1.41	66.2	67.5	67.73	1.02	1.00
17	SHS 160×4.5	3800	136,763	1478.95	1.00	1.21	322.0	318.0	361.82	1.12	1.14

Figures

Fig. 1 3D overview of the Abaqus finite-element model

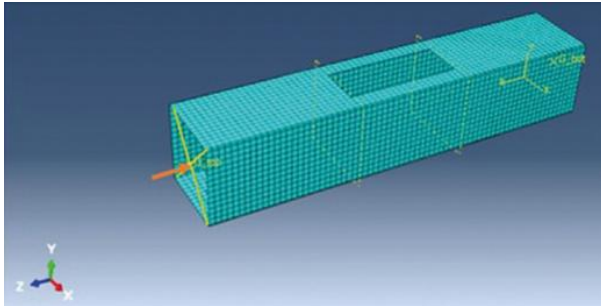


Fig. 2 Comparison of the numerical results with the buckling design curve of EN 1993-1-5 for full cross-sections subjected to pure compression

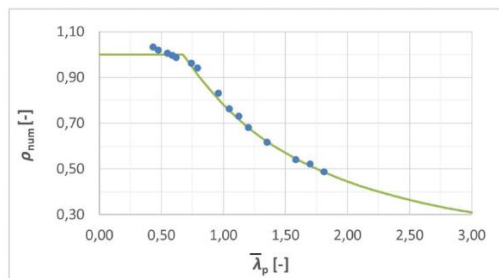


Fig. 3 Static system, bending moment diagram and gross/full and cut and effective cross-sections for centrally loaded short columns

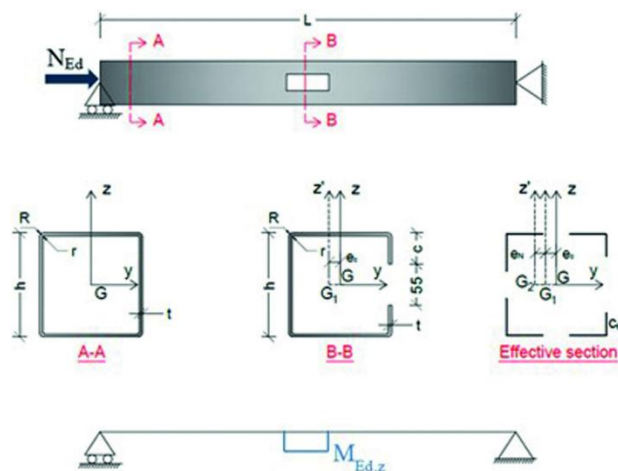


Fig. 4 Comparison of the numerical and analytical sectional resistances for case 1 (centrally loaded short columns)

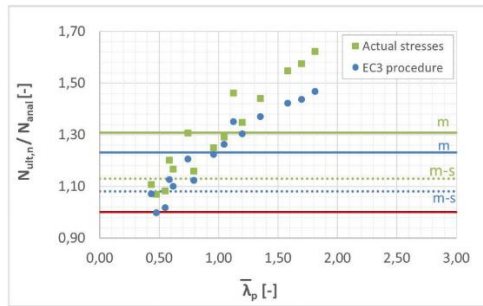


Fig. 5 Comparison of the numerical and analytical sectional resistances for case 2 (eccentrically loaded short columns)

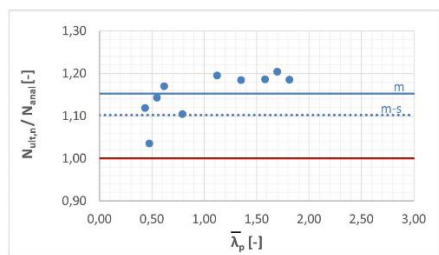


Fig. 6 Layout, geometry details and notations of the studied columns

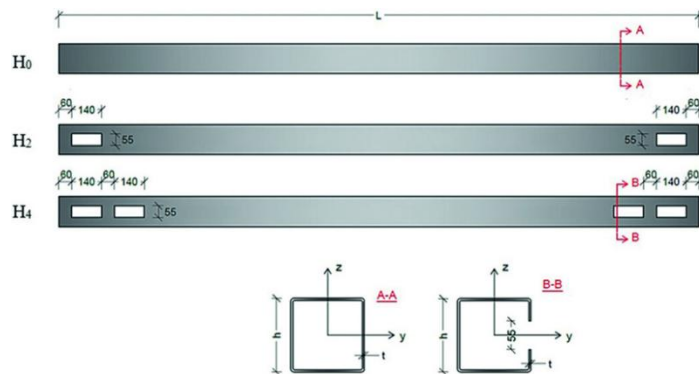


Fig. 7 Comparison of the numerical results of full cross-section members subjected to pure compression with the buckling curves of EN 1993-1-1

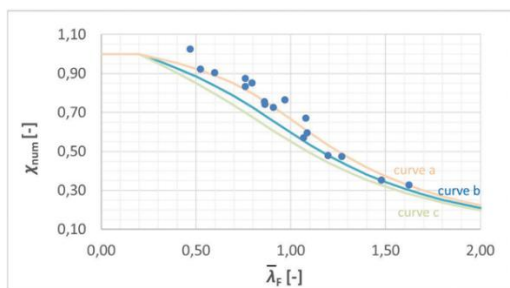


Fig. 8 Comparison of the numerically and analytically determined resistances of members with full cross-section subjected to compression and bending according to both EN 1993-1-3 and prEN 1993-1-3

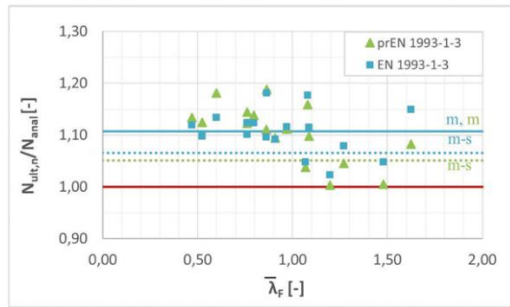


Fig. 9 Comparison of the numerical resistances for members with and without handholes for centrally loaded members subjected to compression

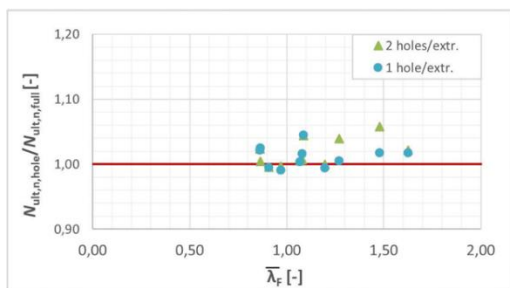


Fig. 10 Comparison of the numerical and analytical buckling resistances for members with handholes at their extremities subjected to compression

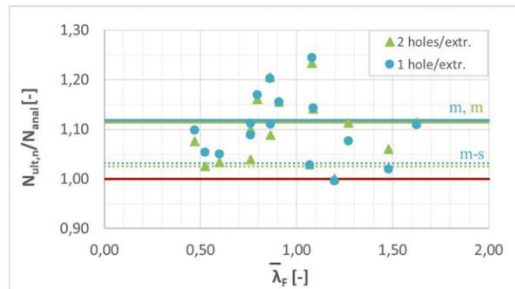


Fig. 11 Comparison of the numerical resistances for members with and without handholes for eccentrically loaded members

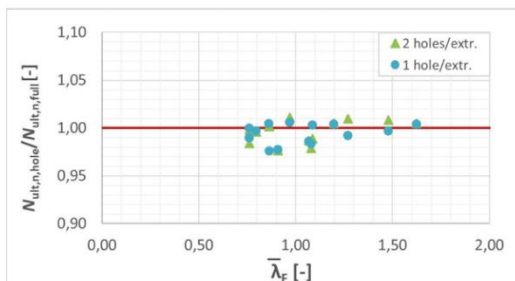


Fig. 12 Comparison of the numerical resistances for members with 1 hole/extremity with the analytical ones evaluated according to both EN 1993-1-3 and prEN 1993-1-3

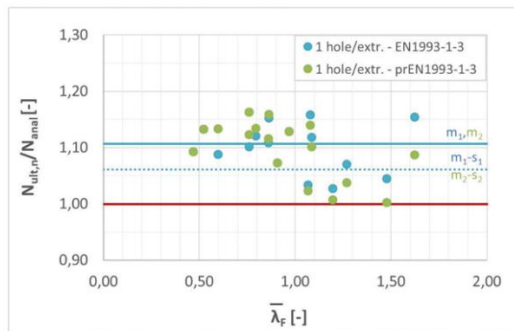
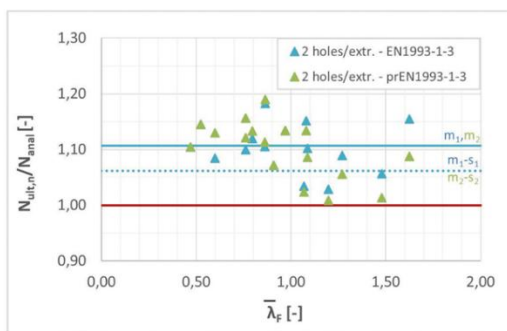


Fig. 13 Comparison of the numerical resistances for members with 2 holes/extremity with the analytical ones evaluated according to both EN 1993-1-3 and prEN 1993-1-3



References

- [1] Toffolon, A.; Müller, A.; Niko, I.; Taras, A. (2019) *Experimental and numerical analysis of the local and interactive buckling behaviour of hollow sections*. ce/papers 3, No. 3-4, pp. 877– 882. <https://doi.org/10.1002/cepa.1148>
- [2] Toffolon, A.; Taras, A. (2019) *Proposal of a design curve for the overall resistance of cold formed RHS and SHS members*. ce/papers 3, no. 3-4, pp. 517–522. <https://doi.org/10.1002/cepa.109>
- [3] Yun, X.; Meng, X.; Gardner, L. (2022) *Design of cold-formed steel SHS and RHS beam-columns considering the influence of steel grade*. Thin-Walled Structures 171, p. 108600.
- [4] Li, S. H. et al. (2009) *Residual stresses in roll-formed square hollow sections*. Thin-Walled Structures 47, pp. 505–513.
- [5] HOLLOSTAB. *Overall-slenderness based direct design for strength and stability of innovative hollow sections*. Research Program of the Research Fund for Coal and Steel, Grant Agreement Number: RFCS-2015-709892.
- [6] Singh, T.; Chan, T.-M. (2021) *Effect of access openings on the buckling performance of square hollow section module stub columns*. Journal of Constructional Steel Research 177, p. 106438.
- [7] Devi, S.; Singh, T.; Singh, K. (2019) *Cold-formed steel square hollow members with circular perforations subjected to torsion*. Journal of Constructional Steel Research 162, p. 105730.
- [8] ABAQUS (2014) *User's Manual, Version 6.14*. Simulia Corp., Providence, RI, USA.
- [9] EN 1993-1-3 (2006) *Design of steel structures – Part 1-3: General rules – Supplementary rules for cold-formed members and sheeting*. Brussels: Comité Européen de Normalisation.

- [10] EN 1993-1-1 (2005) *Design of steel structures – Part 1-1: General rules and rules for buildings*. Brussels: Comité Européen de Normalisation.
- [11] EN 1993-1-5 (2006) *Design of steel structures – Part 1-5: Plate structural elements*. Brussels: Comité Européen de Normalisation.
- [12] prEN 1993-1-3 (2020) *Design of steel structures – Part 1-3: General rules – Supplementary rules for cold-formed members and sheeting*. Brussels: Comité Européen de Normalisation.
- [13] EN 10346 (2009) *Continuously hot-dip coated steel flat products – Technical delivery conditions*. Brussels: Comité Européen de Normalisation.
- [14] Muller, A.; Vild, M.; Taras, A. (2023) *Decision tree for local + global imperfection combinations in double-symmetric prismatic members*. *Steel Construction* 16, No. 1, pp. 2–15. <https://doi.org/10.1002/stco.202200041>
- [15] Rusch, A.; Lindner, J. (2001) *Überprüfung der grenz (b/t)Werte für das Verfahren Elastisch-Plastisch*. *Stahlbau* 70, pp. 857–868.
- [16] CEN/TR 1993-1-103 (2019) *Design of steel structures – Part 1103: Elastic critical buckling of members*. Brussels: Comité Européen de Normalisation (CEN).
- [17] AISI (2016) *American specification for the design of coldformed steel structural members – Appendix 1 – Design of cold-formed members using the direct strength method*. Washington DC: American Iron and Steel Institute.
- [18] Shafer, B. W. (2008) *Review: The direct strength method of cold-formed steel member design*. *Journal of Structural Engineering* 64, pp. 669–679.
- [19] Rondal, J. et al. (1992) *Structural stability of hollow sections. CIDECT, Construction with hollow sections*. Köln, Germany: Verlag TÜV Rheinland GmbH.